Water-Soluble Copolymers. 40. Photophysical Studies of the Solution Behavior of Associative Pyrenesulfonamide-Labeled Polyacrylamides

Stephen A. Ezzell,† Charles E. Hoyle, David Creed, and Charles L. McCormick*

Departments of Polymer Science, Chemistry, and Biochemistry, University of Southern Mississippi, Hattiesburg, Mississippi 39406-0076

Received August 14, 1991; Revised Manuscript Received December 10, 1991

ABSTRACT: Photophysical studies were conducted on copolymers of acrylamide containing less than 0.5 mol % *N*-[(1-pyrenylsulfonamido)ethyl]acrylamide in order to relate the aqueous solution behavior to the molecular structure. The copolymer prepared via a surfactant technique was shown to possess some inherent blockiness or short runs of the pyrenesulfonamide label in dilute solution. Intermolecular associations were observed above a critical concentration of polymer. I_e/I_m values from steady-state fluorescence paralleled the rheological response as a function of concentration. The copolymer prepared by solution polymerization showed random incorporation of the pyrenesulfonamide comonomer and no intermolecular association tendency over the concentration range studied. The pyrenesulfonamide labels were shown to form ground-state aggregates within relatively accessible hydrophilic environments in both polymers. Associative thickening behavior observed in the surfactant-polymerized copolymer is consistent with microphase organization of hydrophobic pyrenesulfonamide aggregates above a critical concentration. Fluorescence quenching has been used to probe the microenvironment around the label.

Introduction

The polymer solution behavior of polyelectrolytes has previously been elucidated via photophysical studies of pyrene-labeled water-soluble polymers including polyelectrolytes,[1-5] poly(ethylene oxide),[6] (hydroxypropyl)cellulose,[7-11] and poly(*N*-isopropylacrylamide).[12,36,37] Particularly relevant work includes that of Winnik et al.,[7-10] who studied pyrene-labeled (hydroxypropyl)celluloses which serve as model associative thickeners. Photophysical analysis demonstrated the aggregation of neutral hydrophobic polymers in aqueous media[7-10] and the interaction with surfactants[10,11] at the molecular level. Frank et al.,[6] investigating pyrene-end-labeled poly(ethylene glycol) (PEG) in aqueous media, showed the associative behavior at the molecular level via the photophysical response of the pyrene label. Molecular aspects of poly(ethylene glycol)/poly(methyl methacrylate) polymer complexation have also been reported.[13-15]

In this study, we have employed photophysical techniques and model compounds to analyze the molecular solution behavior of previously reported pyrenesulfonamide-labeled polyacrylamides which display associative behavior in aqueous media[35] (Chart I). Copolymer 1 was synthesized by a surfactant or "micellar" technique and copolymer 2 in homogeneous solution using a cosolvent. Our goal is to correlate molecular solution behavior with macroscopic solution viscosity response in order to develop overall structure–property relationships for associative water-soluble polymers.

Experimental Section

Materials. Deionized water used in these studies had a conductance of less than 1×10^{-7} mho/cm. Cetylpyridinium chloride was recrystallized from methanol/diethyl ether. Nitromethane was distilled at atmospheric pressure. Other starting materials were purchased commercially and used as received.

Labeled Polymers and Model Compounds (Chart I). The syntheses of pyrenesulfonamide-labeled copolymers 1 and 2 and model compounds 3 and 4 are described in the previous paper in this issue.[35] Labeled copolymer 1 was prepared via a surfactant copolymerization technique and contains 0.25 mol % pyrenesulfonamide label. Copolymer 2 was synthesized via a solution copolymerization technique and contains 0.35 mol % pyrenesulfonamide label.

Synthesis of the Fluorescence Quencher *N*-Methylpyridinium Chloride. The method of Nakaro et al.[16] was modified. The basic procedure involves synthesis of *N*-methylpyridinium iodide with subsequent ion exchange to give *N*-methylpyridinium chloride.

***N*-Methylpyridinium Iodide.** Anhydrous pyridine (26 mL, 25 g, 0.32 mol), was added to diethyl ether (250 mL). Methyl iodide (39 mL, 0.63 mol) in diethyl ether (50 mL) was added dropwise with stirring to the pyridine solution. After the addition was completed, the addition funnel was replaced with a condenser. Refluxing overnight resulted in a white solid precipitate. *N*-Methylpyridinium iodide is very hygroscopic; therefore, purification was accomplished by washing with multiple portions of diethyl ether under N_2. The ether washings were removed via a filter stick,[17] which allowed a continuous inert atmosphere to be maintained. Vacuum drying at room temperature overnight gave a white solid, yield 53 g (76%).

***N*-Methylpyridinium Chloride.** *N*-Methylpyridinium iodide (39 g, 0.16 mol) and silver chloride (35 g, 0.26 mol) were added to water (50 mL). This suspension was allowed to stir overnight in the dark under a nitrogen blanket. Filtration removed the lime-green silver iodide; the filter cake was washed with additional water (25 mL). To ensure completeness of exchange, the aqueous solution was then passed through a column containing Bio-Rad AG 1-X8 ion-exchange resin (10 cm^3, quaternary ammonium type, chloride form). The aqueous effluent tested negative for iodide (persulfate test) and positive for chloride (silver nitrate test). Freeze-drying of the aqueous solution produced a syrup, which was further dehydrated via azeotropic distillation with toluene. The resulting off-white solid mass was extremely hygroscopic; a nitrogen atmosphere was consistently maintained during all manipulations. Residual toluene was removed via a filter stick. Recrystallization from the minimum amount of boiling anhydrous 1-propanol gave *N*-methylpyridinium chloride as white crystals, which were washed with diethyl ether and vacuum-dried at room temperature. All weighings and transfers of this material as a solid were performed under dry nitrogen; storage was over phosphorus pentoxide. Elemental analysis of this compound indicated that 8.15% H_2O was retained. Recovery: 18 g (88%).

† Present address: 3M Science Research Laboratory, St. Paul, MN 55144-1000.

0024-9297/92/2225-1887$03.00/0

Chart I
Pyrenesulfonamide-Labeled Polymers and Model Compounds of This Study

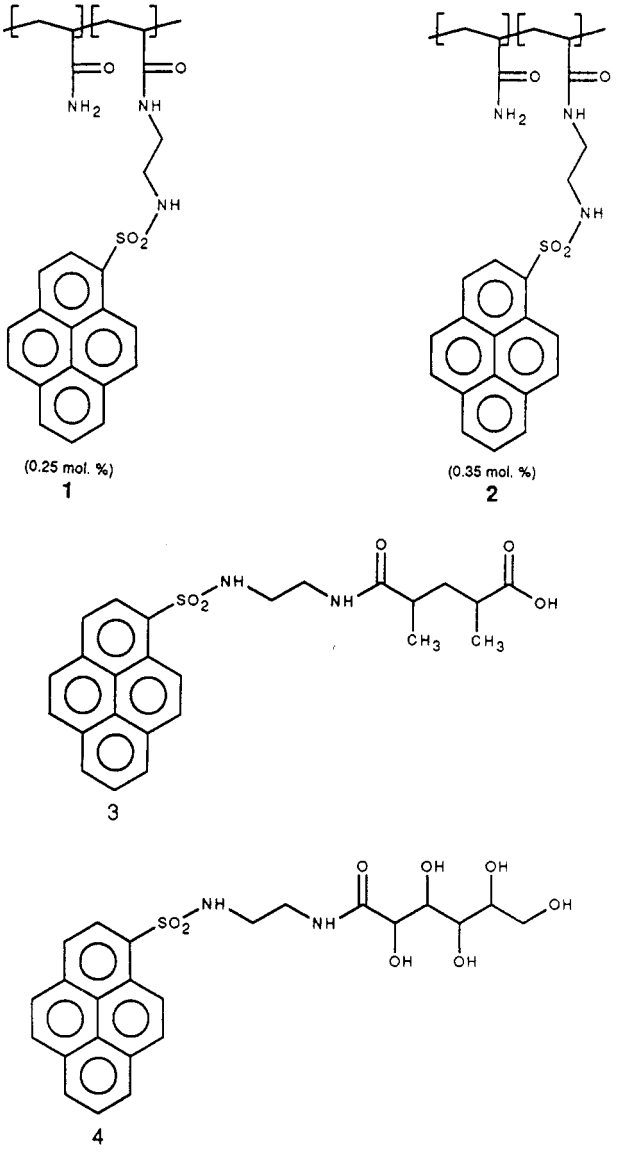

Mp: 138–140 °C (sealed tube). Anal. Calcd: C, 50.87; H, 6.99; Cl, 25.03; N, 9.88. Found: C, 50.58; H, 6.77; Cl, 24.66; N, 9.84. ^{13}C NMR (D_2O, TMS insert): δ 48.25 (CH_3); 128.04, 145.07, 145.30 (aromatic resonances). ^1H NMR (D_2O, TMS insert): δ 3.68 (CH_3); 7.33, 7.80, 8.07 (aromatic CH).

Polymer Characterization. General Procedures. Solution Preparation. Polymer stock solutions were prepared in water or 2% (w/w) aqueous sodium chloride at ca. 200 mg/dL. Several weeks of constant mechanical shaking were required for complete solubilization. Stock solutions were filtered through an 8-μm filter; a peristaltic pump was employed to pump the solution at a low flow rate. Dilution of stock solutions was performed gravimetrically. Samples were allowed to equilibrate for a minimum of 1 week with constant mechanical shaking before characterization.

Characterization. Characterization techniques (other than photophysical) are described in the previous paper in this issue.[35]

Pyrenesulfonamide-Labeled Polymers and Model Compounds. Photophysical Characterization. Steady-State Fluorescence Studies. Steady-state emission studies were performed on a Spex Fluorolog-2 fluorescence spectrometer equipped with a DM3000F data system. All samples were run in the front-face mode to avoid inner filter effects. Slit widths were varied from 0.5 to 2.5 nm, depending on sample concentration. Samples were deaerated by bubbling with nitrogen for 25–30 min. Particularly "foamy" samples were sparged by first bubbling with helium and then with argon. Excitation spectra were obtained via excitation from 250 to 400 nm while monitoring the emission intensity at either 418 nm (monomer emission) or 510 nm (excimer emission). Wavelength-dependent variations in lamp intensity were corrected by an instrumental correction function; Rhodamine B was the internal reference. Detector and emission grating variations were also corrected via an internal function.

Steady-State Fluorescence Quenching. Approximately 200 mg of sample solution were degassed in a septum-capped fluorescence cuvette; a quencher solution was likewise degassed. The emission spectrum was then recorded as described previously. Intensities of the (0,2) (monomer, 400 nm) band were recorded in the absence of quencher (I_0). A microliter syringe was used to deliver aliquots, generally 1–3 μL, of the quencher solution to the sample. The sample cuvette was shaken, and the diminished values of fluorescence intensity were recorded. A positive inert gas pressure was maintained in both the cuvette and quencher vials in order to exclude oxygen.

Transient Fluorescence Studies. A Photochemical Research Associates (PRA) single-photon-counting instrument equipped with a H_2-filled 510-B flashlamp was used to obtain fluorescence decay curves. Fluorescence decay times were fit from decay profiles using either a Digital Micro PDP-11 or an IBM PC. In either case, PRA software was used which employs a nonlinear iterative deconvolution technique to analyze decay curves.

Sample degassing was as described previously. Pyrenesulfonamide-labeled materials were excited at 340 nm; decays were measured at 400 nm (monomer emission) or 519 nm (excimer emission). We have found it important to use a minimal time-per-channel setting to avoid placement of counts in the lower time decades. An appropriate setting for these materials is 0.1786 ns/channel for a range of 512 channels; 10^4 counts were generally taken in the maximum channel.

Transient Fluorescence Quenching Studies. Sample handling was as described for the steady-state quenching experiments, except 400 mg of sample solution was employed. Excitation was at 340 nm; fluorescence decay profiles of the 400-nm (monomer) band were obtained as a function of the quencher concentration.

Results and Discussion

Model Compound Photophysics. To assist in analyzing the photophysical properties of synthetic copolymers 1 and 2 containing the pyrenesulfonamide monomer, we prepare water-soluble model compounds 3 and 4 with the pyrenesulfonamide chromophore. The solubility of compound 4 in water is limited to 3×10^{-5} M despite the hydrophilic gluconamide group. Likewise the solubility of 3 is 6×10^{-5} M at pH 7. At higher pH values the salt is more soluble (1×10^{-2} M).

The UV absorption spectra of 3 and 4 in deionized H_2O are displayed in Figure 1 for comparative purposes. These spectra are essentially identical, as would be expected since both possess the same chromophore. Steady-state fluorescence spectra of 3 and 4 (Figure 2) were recorded upon excitation at 340 nm, over the range 350–600 nm. The three peak maxima characteristic of the monomer emission are 380 (0,0), 400 (0,2), and 418 nm (0,3). In the concentration regime employed (10^{-5} M), the solutions are sufficiently dilute to preclude the formation of excimer. The fluorescence spectrum of a concentrated (ca. 10^{-2} M) aqueous solution of the sodium salt of 3 is shown in Figure 3. The structureless red-shifted emission centered at about 520 nm can be assigned to excimer which forms at higher concentration levels. It should be noted that the salt of 3 may have surfactant characteristics which contribute to excimer formation.

The sulfonamide proton of the pyrenesulfonamide group is acidic; sulfonamides typically have pK_a values ranging from 10 to 12. The effect of pH on the emission was examined by recording fluorescence spectra of 3 (6×10^{-5}

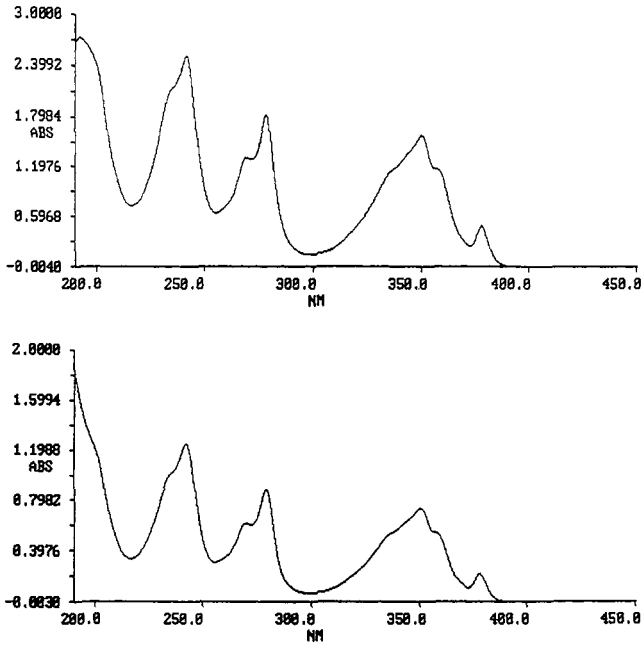

Figure 1. UV absorption spectra of **3** (top) and **4** (bottom) in deionized H_2O (C = 10^{-5} M).

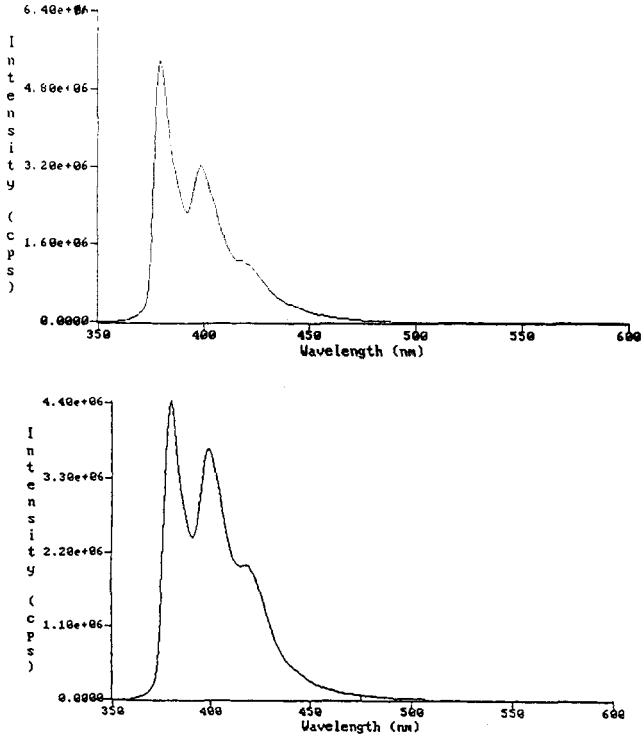

Figure 2. Steady-state fluorescence spectra of **3** (top) and **4** (bottom) in deionized H_2O (C = 10^{-5} M).

M) at pH 10.6 and 12.1. The intensity of the spectrum at pH 12.1 was one-third of that at pH 10.6. The spectral shapes were identical. The diminished intensity of the spectrum acquired at higher pH is likely due to a lack of fluorescence from the sulfonamide anion. Use of this label as a fluorescent tag must therefore be limited to media of pH < 10.

Polymer Absorption and Steady-State Emission Spectra. UV Absorption Spectrum. Figure 4 shows the UV absorption spectra of pyrenesulfonamide-labeled polymers **1** and **2** in deionized H_2O. The absorption spectra above 220 nm are qualitatively identical to those for the model compounds **3** and **4** in Figure 1. This is evidence that the pyrenesulfonamide label has maintained its

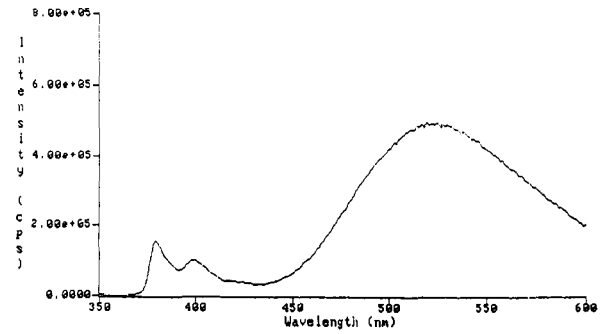

Figure 3. Steady-state emission spectrum of **3** (sodium salt, C = ca. 10^{-2} M) in deionized H_2O.

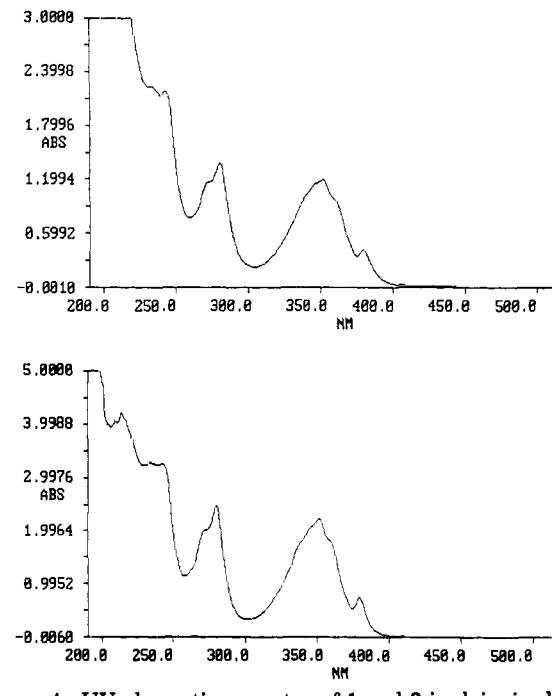

Figure 4. UV absorption spectra of **1** and **2** in deionized H_2O (C = 0.15 g/dL).

integrity during the polymerization process. However, the polymer absorption spectra in Figure 4 are red-shifted compared to those of the model compounds (Figure 1). Comparison of Figures 1 and 4 reveals that the polymer absorption extends to 400 nm; the model compounds, however, fail to absorb appreciably at wavelengths longer than 390 nm. The significance of this effect will be further discussed in a later section.

Steady-State Emission. Steady-state emission spectra of surfactant-polymerized **1** and solution-polymerized **2** are shown in Figure 5. Both labeled polymers display the three peaks assigned to monomer emission, as shown for the model compounds in Figure 2. Excimer emission—centered around 519 nm—is also observed for the labeled polymers. Excimer emission is definitely a polymer-enhanced effect, since the content of the label is 7×10^{-5} M for copolymer **1** and 9×10^{-5} M for copolymer **2**. No excimer intensity was observed for the model compounds in this concentration range (Figure 2).

Although **2** contains slightly more pyrenesulfonamide label (0.35 mol % for **2** and 0.25 mol % for **1**), the excimer emission intensity of **1** is dramatically enhanced relative to **2**. A greater *local concentration* of the label therefore exists for **1** relative to **2**, strongly suggesting that microstructural differences exist between these polymers. We believe that copolymer **2**, prepared in homogeneous solution, has a more random structure than surfactant-

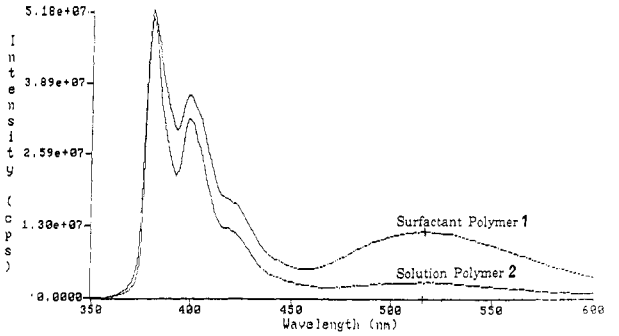

Figure 5. Steady-state emission spectra of 1 (copolymer C = 218 mg/dL; fluorophore $C = 7.13 \times 10^{-5}$ mol L) and 2 (copolymer C = 193 mg/dL; fluorophore $C = 9.28 \times 10^{-5}$ mol/L) in deionized H_2O.

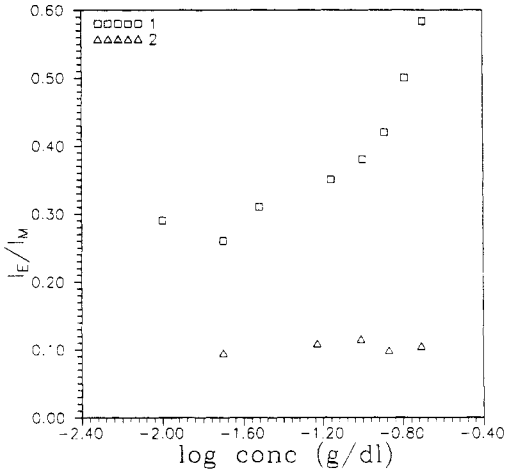

Figure 6. I_E/I_M as a function of the log concentration of 1 and 2 in deionized H_2O.

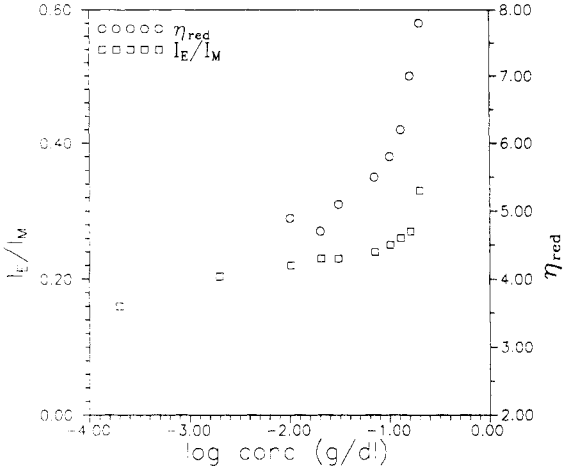

Figure 7. η_{red} and I_E/I_M as a function of the log concentration for 1 in deionized H_2O.

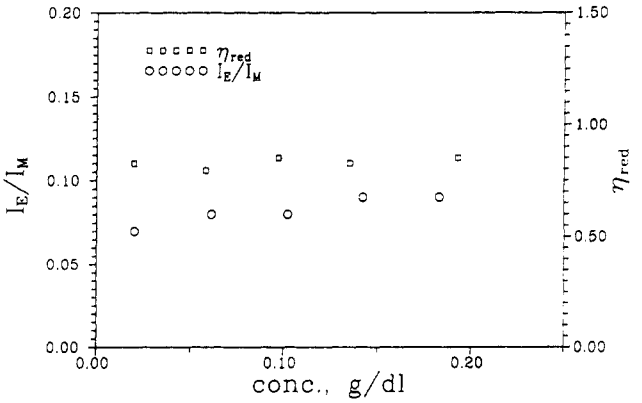

Figure 8. η_{red} and I_E/I_M as a function of the concentration for 2 in deionized H_2O.

polymerized 1, which possesses a blocky microstructure.[35] The microheterogeneous surfactant produces partitioning of the hydrophobic pyrenesulfonamide monomer within the micelle during copolymerization, allowing some degree of blockiness even at low feed composition. Clearly the number of consecutive pyrenesulfonamide label repeat units is determined to some extent by the pyrenesulfonamide monomer label-to-surfactant ratio. Effects of surfactant polymerization methods upon the polymer microstructure have been noted elsewhere. In separate studies, Peer[18] and Dowling and Thomas[19] investigated copolymers synthesized from acrylamide and a hydrophobic comonomer by a surfactant copolymerization technique. The microstructures of these systems are also believed to have blocky characteristics. The copolymers demonstrated either intra- or intermolecular solution behavior,[18] apparently depending upon the choice of hydrophobic comonomer, polymerization conditions, and other factors.

The concentration dependence of excimer-to-monomer ratios, I_E/I_M, for the two copolymers is shown in Figure 6. The concentrations of the polymers were viewed over a range of 10^3, from 2.0×10^{-4} to 0.2 g/dL. The concentration dependences of I_E/I_M values are dramatically different. The I_E/I_M values for 2, the polymer synthesized in homogeneous solution, show only a small concentration dependence, signifying little or no change in the pyrene environment and therefore in polymer conformation. However, I_E/I_M values for 1, the polymer synthesized in the presence of surfactant, increase dramatically at concentrations above ca. 0.1 g/dL, indicating that the pyrene groups are in an increasingly hydrophobic environment presumably caused by increasing intermolecular associations.

The increases of I_E/I_M values with polymer concentration (Figure 6) are paralleled by changes in viscosity, a bulk or macroscopic property. In Figure 7, I_E/I_M and the reduced viscosity of copolymer 1 are plotted as a function of concentration. Viscosity and I_E/I_m *both* increase dramatically above an initial concentration, C^* (ca. 0.1 g/dL), providing strong evidence that intermolecular hydrophobic associations of the pyrenesulfonamide labels are responsible. As concentration increases, intermolecular hydrophobic association of the labels is facilitated. It has been proposed that hydrophobic molecules can locate each other at distances greater than 100 Å due to the strong influence of water-structuring.[20-22] This is reflected on a molecular level by enhancement of I_E/I_M values. On a macroscopic scale, hydrophobic associations are indicated by a sharp increase in the viscosity profile at C^*. To our knowledge, this represents the first associative thickener which relies on a fluorescence label as the sole hydrophobic moiety. Also, the parallel response of I_E/I_M and η_{red} vs concentration (Figure 8), along with previous literature studies, allows rational suggestions to be made on the mode of the micellar or surfactant polymerization, as well as the nature of the aggregation responsible for the associative thickening phenomenon.

Concentration dependencies of η_{red} and I_E/I_M are shown in Figure 8 for copolymer 2 prepared in DMF/H_2O. The zero Huggins constant of the reduced viscosity vs concentration curve suggests a compact polymer conformation that is independent of polymer concentration. The I_E/I_M values confirm this premise. The microstructure of this

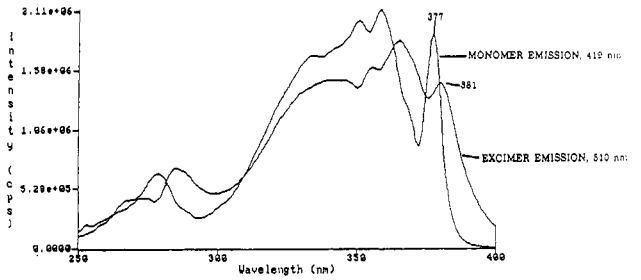

Figure 9. Excitation spectrum at monomer and excimer emissions of 1 in deionized H_2O, C = 0.22 g/dL.

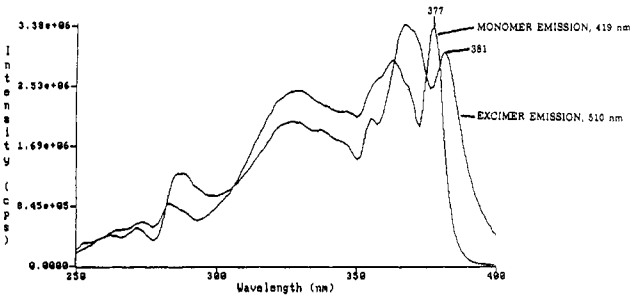

Figure 10. Excitation spectrum at monomer and excimer emissions of 2 in deionized H_2O, C = 0.19 g/dL.

polymer—random label distribution—no doubt strongly influences the polymer conformation. In water, the hydrophobic labels are compelled to aggregate by the hydrophobic effect. The random interspacing of the hydrophobe along the polymer backbone leads to compaction of the polymer coil due to intramolecular associations. Such a compact structure is reflected in the viscosity profile of 2, as we have shown.

In order to further elucidate the nature of the hydrophobic associates, additional studies were conducted. Excitation spectra for polymers 1 and 2 are shown in Figures 9 and 10, wherein emission was monitored at both monomer (419 nm) and excimer (510 nm) wavelengths. In each case, the excitation spectrum of the excimer emission is red-shifted by 4 nm from the monomer excitation spectrum. This suggests that preformed, ground-state aggregates of the pyrenesulfonamide labels are the source of excimer emission. The loss of vibrational structure is consistent with ground-state association.

Typically, in polymer systems, excimer emission results from chromophores which encounter one another through a diffusional process. A chromophore absorbs light, is promoted to the excited state, and, during its excited-state lifetime, encounters a ground-state chromophore. In this case, monomer and excimer excitation spectra are identical, since the initial absorbing species are identical. In our case, however, hydrophobic associations of the pyrenesulfonamide label appear to facilitate the formation of ground-state aggregates. Hydrophobic interactions of the pyrenesulfonamide labels provide a means for facilitating perturbation of the ground state and yielding a species of lower energy. This results in a red-shift in both the absorption spectrum and the excitation spectrum when emission is monitored in the excimer or, perhaps more appropriately, excited aggregate region.

The phenomenon of pyrene absorption and excitation spectral shifts in the context of ground-state interactions has been previously documented. In a fundamental study, Avis and Porter[23] examined the photophysics of pyrene dissolved in a poly(methyl methacrylate) matrix as a function of pyrene concentration. At pyrene concentrations ≥0.01 mol dm^{-3}, excimer emission was observed and

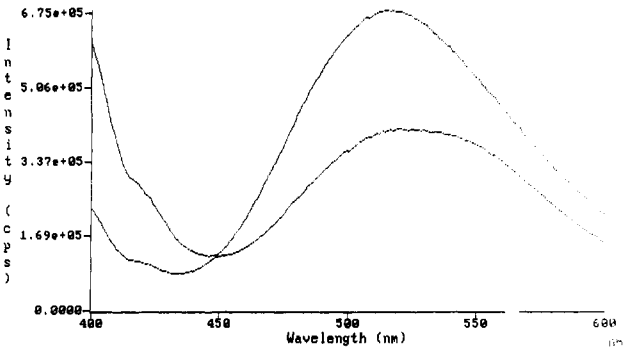

Figure 11. Steady-state emission spectra of 1 and 2 in deionized H_2O (excitation of aggregates at 395 ± 1 nm); concentrations as in Figure 5.

absorption and excitation spectra were red-shifted relative to the spectra of pyrene at lower concentrations. van der Waals interactions of proximate pyrene molecules, resulting in aggregates of lower ground-state energy, were proposed to explain the observed spectral shifts.

Precedence also exists for the aggregation of pyrene-labeled, water-soluble polymers in aqueous media. Winnik and co-workers[7-10] have studied the aggregation behavior of pyrene-labeled (hydroxypropyl)celluloses in water. Excimer excitation spectra were red-shifted relative to monomer excitation spectra, indicating ground-state interactions of the pyrene labels. No rise times were observed for the decay profiles, verifying the preformed nature of the aggregate. Frank and co-workers[6] have reported similar results for pyrene-end-labeled poly(ethylene glycol) in H_2O. In both Winnik's and Frank's studies, comparative spectroscopic studies of pyrene-labeled polymers were performed in methanol as well as in water. No ground-state aggregation of the label moieties was observed in methanol, thus emphasizing the importance of the hydrophobic effect.

Additional evidence for aggregation in polymers 1 and 2 was obtained by excitation of aqueous solutions of 1 and 2 (Figure 11) at 395 nm. Emission in the monomer region is very low for both polymers (compare with Figure 6). The broad red-shifted emission dominates, indicating that indeed the pyrene aggregate is responsible for excimer emission in solutions of 1 and 2. The small amount of monomer emission which seems to be present could be due in part to dissociation of the excited aggregate.

Transient Emission Studies. Analysis of Transient Decay. Background. The Birks[24,25] scheme for excimer formation/dissociation indicates that monomer fluorescence decays as the sum of two exponential terms while the excimer decay can be described as the difference of two exponential terms. The Birks kinetic scheme adequately describes the transient decay behavior of low molar mass systems and some model polymer systems. However, many labeled polymer systems exhibit a complex decay response, and this has been our experience with both 1 and 2.

The fluorescence decay profiles of the models in water or dioxane are monoexponential (Table I). The difference in the lifetimes in water (ca. 13 ns) and dioxane (ca. 30 ns) is quite large, demonstrating the effect of microenvironmental polarity on the decay of the excited state.

The decay profiles of the two polymers 1 and 2 in aqueous solution were complex but could be approximately fit by a sum of two exponentials. In both cases, the decay curve could be fit to a longer-lived component (ca. 15 ns) and a shorter-lived component (ca. 11 ns). Detailed interpretation is impossible, probably because labels in many

Table I
Fluorescence Lifetimes of Model Compounds in Homogeneous Solution[a]

sample	solvent	C, M	T, ns
3	H_2O	2.5×10^{-7}	13.3
	dioxane	2.6×10^{-7}	30.9
4	H_2O	3.1×10^{-7}	13.1
	dioxane	3.1×10^{-7}	30.3

[a] Excitation at 340 nm; monitoring at 400 nm.

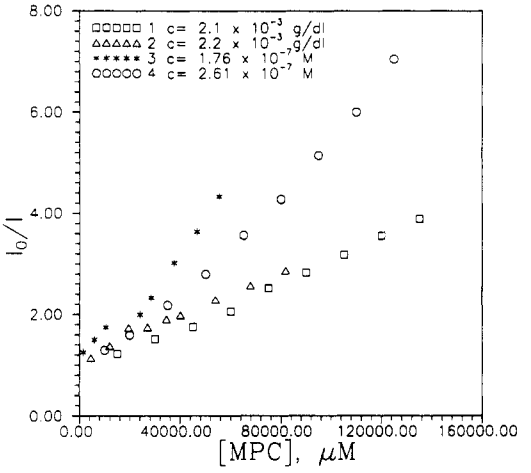

Figure 12. MPC quenching of pyrenesulfonamide polymers and models.

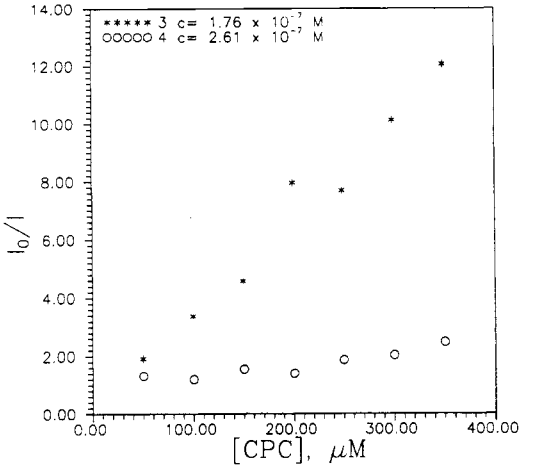

Figure 13. CPC quenching of pyrenesulfonamide models (label concentration $\approx 10^{-5}$ M).

different environments are contributing to the emission decay. One point, however, is particularly informative. The decay profile of the monomer emission (400 nm) of 1 is invariant, within experimental error, with change in the concentration from 2.2×10^{-3} to 2.2×10^{-1} g/dL. However, as noted previously, both the reduced viscosity and the I_E/I_M ratio of 1 increase at concentrations on the order of 2.2×10^{-1} g/dL (Figure 7). It appears as though the local environment of the species responsible for emission at 400 nm in 1 is modified little, if at all, as polymer aggregation occurs.

While it is difficult to interpret the excimer decay profile of the polymer samples, it is worth noting that the excimer decay profiles of 1 and 2 obtained at 550 nm do not exhibit a rise time (characteristic of the diffusion time for excimer formation). The rise times at 550 nm (excimer or excited aggregate emission region) and 400 nm (monomer emission region) are essentially identical. Although specific decay times were not obtained, in general, we note that the decay profile has a long-lived decay component

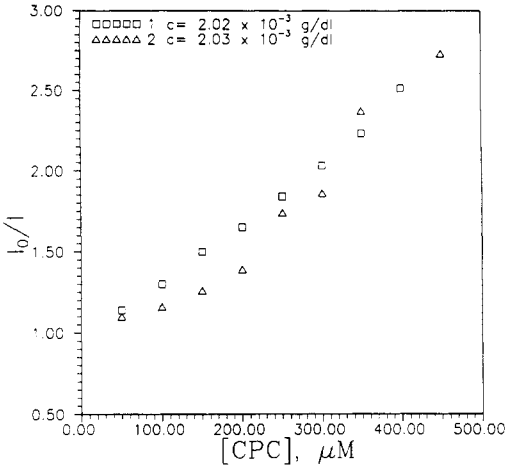

Figure 14. CPC quenching of pyrenesulfonamide polymers (label concentration $\approx 10^{-7}$ M).

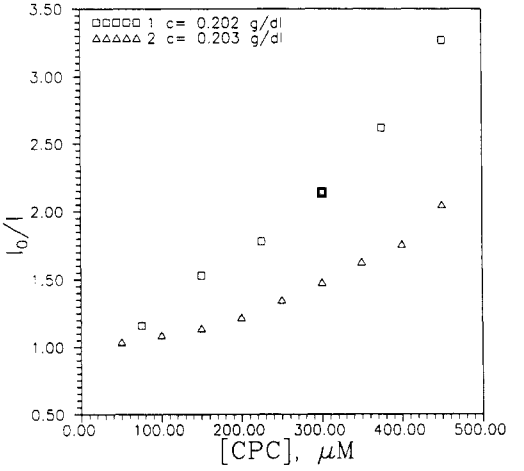

Figure 15. CPC quenching of pyrenesulfonamide polymers (label concentration $\approx 10^{-4}$ M).

on the order of 30 ns. The decay profiles in the excimer region suggest the presence of a ground-state dimer. This idea is supported by the work of Wang et al.,[26] who performed picosecond excimer fluorescence spectroscopy on poly(1-pyrenylmethyl methacrylate) in chloroform. In this study an essentially instantaneous rise was observed for the excimer fluorescence profile on a picosecond time scale, signifying ground-state interactions of the pendent pyrene moieties.

For pyrene-labeled (hydroxypropyl)cellulose, Winnik et al.[7] also identified ground-state pyrene aggregates via excitation spectra and the lack of a rise time for the excimer decay. Frank and co-workers[27] also attributed the emission of pyrene-end-labeled PEG to excitation of preformed pyrene aggregates.

Quenching Studies. In order to further probe the microenvironment of the pyrene fluorophore, the fluorescence of the polymers and the model compounds was quenched by nitromethane (N), iodide ion (I), methylpyridinium chloride (MPC), and cetylpyridinium chloride (CPC). In the case of N and I, quenching data fit the Stern–Volmer equation (eq 1),

$$I_0/I = 1 + K_{SV}[Q] \quad (1)$$

where $K_{SV} = k_Q\tau_0$, I_0 = emission intensity in the absence of quencher, Q, I = emission intensity in the presence of Q, [Q] = quencher concentration, K_{SV} = Stern–Volmer quenching constant, k_Q = quenching rate constant, and τ_0 = lifetime of unquenched fluorophore such that plots

Scheme I
Simple Kinetic Model for Static and Dynamic Quenching of a Fluorophore, M, by a Quencher, Q

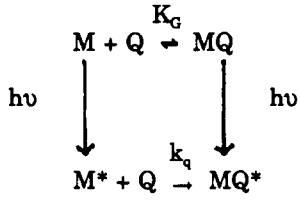

("Stern–Volmer plots") of I_0/I vs [Q] were linear for [Q] < ca. 0.01 M. The same plots for MPC and CPC quenching frequently showed upward curvature (Figures 12–15), even at low concentrations of Q, indicative of both static (complexation of Q to fluorophore) and dynamic quenching processes. Attempts to fit these curved plots using several currently available kinetic treatments[36,37] failed. Thus, we will discuss the results using the *simplest* possible kinetic model (Scheme I) for static plus dynamic quenching of a fluorophore M, by Q, in which K_G is the association constant for formation of the complex, MQ. Provided the extinction coefficients of M and MQ at the wavelength of excitation are the same (i.e., Q does not significantly perturb the absorption spectrum of M), the excited complex MQ* is nonfluorescent, and MQ* does not revert significantly to M*, then the modified Stern–Volmer expression (eq 2) holds.[29] This reduces to eq 3 for purely static quenching ($K_{SV} = 0$). This has the same I_0I vs [Q]

$$I_0/I = 1 + (K_{SV} + K_G)[Q] + K_{SV}K_G[Q]^2 \quad (2)$$

$$I_0/I = 1 + K_G[Q] \quad (3)$$

dependence as purely dynamic quenching but can be distinguished from the latter by measurement of the fluorophore lifetime in the absence (τ_0) and presence (τ) of Q for which eq 4 applies. Thus, for purely dynamic quenching

$$\tau_0/\tau = 1 + K_D[Q] \quad (4)$$

ing $K_{SV} = K_D$, whereas for purely static quenching $K_D = 0$; i.e., the fluorophore lifetime is independent of [Q], although the fluorescence intensity drops as [Q] increases. Finally, from eq 2, the slopes of upwardly curving Stern–Volmer plots should tend to a value of $K_{SV} + K_G$ as [Q] approaches 0.

Stern–Volmer constants (K_{SV}) for the quenching of monomer emission at 400 nm by N, an amphiphilic quencher, and I, an anionic heavy-atom quencher, are given in Table II. From the known lifetimes (τ_0) of the fluorophores (Table I) of the model compounds, both N and I quench fluorophore fluorescence at or near the diffusion-limited rate ($k_Q = (4–7) \times 10^9$ M^{-1} s^{-1}). Exact quenching constants (k_Q) were not calculated for polymers 1 and 2 since a single fluorescence lifetime was not obtained for these materials. However, it is worth noting that K_{SV} values for models 3 and 4 are consistently greater than those for the polymer-bound labels. The (approximately) two-component fluorescence decay of the polymers, with $\tau \simeq 15$ and 11 ns, has a similar "average" lifetime to the single-component decay ($\tau_0 \simeq 13$ ns) of the models (Table I), suggesting k_Q for the polymers is 2–4 times smaller than k_Q for the models. This is attributable to the bulk of the polymers and the enhanced viscosity of the medium. The approximate k_Q values for the polymers (ca. (1–4) × 10^9 M^{-1} s^{-1}) are in the range of being diffusion limited and indicate ready accessibility of these quenchers to the pyrene label.

Table II
Quenching of the Fluorescence[a] of Polymers 1 and 2 and Model Compounds 3 and 4 by Nitromethane (N) and Sodium Iodide (I) in Water

compound	Q	[polymer], g/dL	[label], M	K_{SV}, M^{-1}	k_Q, M^{-1} s^{-1}
3	N		2.5×10^{-8}	49	3.7×10^9
4	N		3.1×10^{-7}	58	4.4×10^9
1	N	2.18×10^{-1}	7.1×10^{-5}	11	
1	N	2.18×10^{-3}	7.1×10^{-7}	23	
2	N	1.93×10^{-1}	9.3×10^{-5}	12	
2	N	1.93×10^{-3}	9.3×10^{-7}	17	
3	I		1.8×10^{-7}	74	5.6×10^9
4	I		2.6×10^{-7}	85	6.5×10^9
1	I	2.0×10^{-3}	6.5×10^{-7}	49	
2	I	2.2×10^{-3}	1.1×10^{-6}	43	

[a] Excitation at 340 nm; quenching at 400 nm.

Table III
Quenching of the Fluorescence[a] of Polymers and Model Compounds by Methylpyridinium Chloride (MPC) and Cetylpyridinium Chloride (CPC) in Water

compound	Q	[polymer], g/dL	[label], M	slope, M^{-1}	K_D, M^{-1}
3	MPC		1.8×10^{-7}	58[b]	
3	CPC		1.8×10^{-7}	35000[b]	
4	MPC		2.6×10^{-7}	36[b]	35
4	CPC		2.6×10^{-7}	4000[b]	60
1	MPC	2.0×10^{-3}	6.5×10^{-7}	18[c]	
2	MPC	2.2×10^{-3}	1.1×10^{-6}	20[c]	
1	CPC	2.0×10^{-3}	6.5×10^{-7}	3800[c]	
2	CPC	2.0×10^{-3}	1.0×10^{-6}	1900[b]	
1	CPC	2.0×10^{-1}	6.5×10^{-5}		
2	CPC	2.0×10^{-1}	1.0×10^{-4}		

[a] Excitation at 340 nm; monitoring at 400 nm. [b] Nonlinear Stern–Volmer plots. The slope is at the linear portion at low Q. [c] Slopes at linear Stern–Volmer plots.

In order to further probe the hydrophobicity of the labeled polymers, CPC, a hydrophobic quencher, was employed for intensity quenching. CPC is a surfactant with a critical micelle concentration (cmc) of 8×10^{-4} M;[28] its pyridinium ring is an oxidative quencher. For comparative purposes, *N*-methylpyridinium chloride (MPC), a less hydrophobic analogue of CPC, was also used.

Figures 12–15 are the monomer intensity quenching curves (Stern–Volmer plots) of the pyrenesulfonamide model compounds and labeled polymers for the alkylpyridinium quenchers. Quenching of the fluorescence of 1 and 2 by CPC is shown for two label concentrations (Figures 14 and 15). In no instance did we observe evidence of exciplex formation in either absorption or emission spectra. Many of the plots show upward curvature. This is probably indicative of a combined static and dynamic quenching process. In the case of MPC quenching of the fluorescence of 3 and 4 (Figure 12), the curvature of the plots is less pronounced than that for CPC, despite the fact that concentrations of MPC were typically over 100 times greater than those for CPC. Stern–Volmer plots for MPC quenching of the fluorescence of 1 and 2 (Figure 12) are essentially linear. In all other cases we estimated the initial slopes of I_0/I vs [Q] plots. Some experiments were also conducted in which fluorophore lifetimes were measured in the presence of Q in order to obtain K_D and k_Q via eq 4.

A summary of the data for fluorescence quenching of 1–4 by MPC and CPC is given in Table III. In the case of the fluorescence of 3 quenched by CPC (Figure 13) a very large initial slope (35 000 M^{-1}) was obtained. This is attributed to complexation of the large hydrophobic carboxylate anion of 3 (a carboxylic acid, but above its

pK) with the large hydrophobic cation CPC. Quenching of the fluorescence of 4 by MPC (Figure 12) must be almost entirely a dynamic process since $K_{SV} \simeq K_D \simeq 35\ M^{-1}$. The quenching rate constant for this process is $2.7 \times 10^9\ M^{-1}\ s^{-1}$ since $\tau_0 = 13.1$ ns for 4 in deionized H_2O (Table I). In contrast, CPC quenching of the fluorescence of 4 (Figure 13) gave an initial slope of $4000\ M^{-1} \gg K_D = 60\ M^{-1}$, indicating a large component of static quenching by CPC. Since 4 is neutral (in contrast to 3), its association with CPC is hydrophobically driven. A hydrophobic salt is formed which is nonfluorescent and leads to predominantly static quenching, in contrast to MPC, which quenches by a purely dynamic mechanism. For CPC quenching of the fluorescence of 4 a value of $k_Q = 4.6 \times 10^9\ M^{-1}\ s^{-1}$ can be obtained from K_D and τ_0. Thus, dynamic quenching of the fluorescence of 4 by both MPC and CPC occurs at near-diffusion-limited rates.

The analysis of MPC and CPC quenching data for the polymers 1 and 2 is hindered by the complex fluorescence decay behavior of the label in the polymer. This precludes our obtaining k_Q values for the polymers using eq 4. However, careful examination of the Stern–Volmer plots of I_0/I vs [Q] leads to some intriguing conclusions. Thus, MPC quenching of the fluorescence of 1 and 2 (Figure 12) gives essentially identical, linear Stern–Volmer plots with slopes of 18 and 20 M^{-1}, respectively. The linear plots indicate either purely dynamic (slope = K_{SV}) or purely static (slope = K_G) quenching. Concentrations of MPC in the same range used for the I_0/I vs [Q] experiments, markedly reduced the (nonexponential) decay of the fluorescence of 1 and 2.[38] Although it is not meaningful to obtain a k_Q value for such a nonexponential decay, this result indicates that MPC quenches the fluorescence of the polymers by a predominantly dynamic, diffusional process. In this respect MPC is analogous to both N and I in its quenching behavior. Once again, the lower values of K_{SV} for polymers 1 and 2 relative to models 3 and 4 can be attributed to the bulk of the polymers and the enhanced viscosity of the medium.

CPC quenching of the fluorescence of low concentrations of 1 and 2 (Figure 14) gives quite a different result from MPC quenching. The Stern–Volmer plot for the surfactant polymer 1 plus CPC is approximately linear with a slope of ca. $3800\ M^{-1}$ for [CPC] < ca. 4×10^{-4} M, whereas the plot for the solution polymer 2 plus CPC is distinctly curved upward over the same range of [CPC] with a much lower initial slope of ca. $1900\ M^{-1}$. The near linear plot for [CPC] and its high slope must be a consequence of predominantly static quenching with $K_G \simeq 3800\ M^{-1}$. Assumption of dynamic quenching (i.e., $K_{SV} \simeq 3800\ M^{-1}$) would lead to an unreasonably high k_Q of ca. $3 \times 10^{11}\ M^{-1}\ s^{-1}$ if $\tau_0 = 13$ ns is assumed for the polymer. Indeed, the slope of $3800\ M^{-1}$ for 1 plus CPC is very similar to the value of $4000\ M^{-1}$ obtained for neutral model 4 plus CPC. We note that the (nonexponential) fluorescence decay is minimally affected by addition of CPC quencher relative to MPC, thus verifying the static nature of the CPC–polymer label interaction.[38] Presumably association of both 1 and 4 with CPC is hydrophobically driven. The solution polymer 2 also gives a large but lower initial slope ($1900\ M^{-1}$) of the Stern–Volmer plot for CPC quenching. The lower initial slope indicates less complexation, and the curvature of the plot suggests a larger contribution of dynamic quenching for this polymer with randomly spaced pyrene labels. Stern–Volmer plots for quenching of the fluorescence of higher concentrations of 1 and 2 by CPC are shown in Figure 15. Both plots show marked upward curvature most probably a consequence of the CPC concentrations (up to 5×10^{-4} M) being comparable to label concentrations. Once again the effect of CPC on the fluorescence of 1 is greater than that on the fluorescence of 2 at low [CPC], suggesting the surfactant quencher interacts more strongly with polymer 1, which has blocks of hydrophobic pyrene labels. Thus hydrophobically modified polymers form (static) hydrophobic aggregates with surfactants such as CPC, even below the critical micelle concentration of the surfactant. Formation of such aggregates is the dominant mechanism of fluorescence quenching by CPC, the effect being most striking for the surfactant polymer 1. Such polymer/surfactant complexes are of interest from both fundamental[30] and practical[31] points of view. It may also be significant that, at low polymer concentrations, K_{SV} for the fluorescence of 1 quenched by CPC is about twice as large as the initial slope for 2 quenched by CPC (recall that K_{SV} values for 1 and 2 plus MPC are essentially identical). This may indicate that the hydrophobic CPC has some preference for association with the blocky regions of 1 rather than the more randomly spaced hydrophobic labels in 2. A number of other groups[1,10,11,32-34] have employed photophysical techniques to observe surfactant interactions with pyrene-labeled polymers. Our study differs in that we have also employed a quenching process to observe these interactions.

Conclusions

This work dealt with the photophysics of pyrenesulfonamide-labeled water-soluble polymers prepared by either a microheterogeneous surfactant copolymerization technique or by a homogeneous solution polymerization technique. The surfactant copolymerization technique yielded a pyrenesulfonamide-labeled copolymer 1, which proved to be a model associative thickener. Viscosity profiles of this polymer in aqueous media exhibit a low critical overlap concentration—typical associative thickener behavior. A blocky microstructural tendency was demonstrated for this polymer from I_E/I_M ratios of the pyrenesulfonamide label. This microstructure is a consequence of the microheterogeneity present during the surfactant copolymerization. Hydrophobic interactions of the label, as evidenced by I_E/I_M, parallel that of the viscosity profile. The viscosity response of the polymer is therefore driven by the molecular, hydrophobic interactions of the pyrenesulfonamide label. These hydrophobic interactions lead to a formation of static, ground-state aggregates of the pyrene labels as denoted by excitation studies and lifetime measurements. Quenching studies of the pyrenesulfonamide label imply that it resides in an open, aqueous environment accessible to hydrophilic quenchers such as iodide ion. The hydrophobic character of the label was verified by its interactions with the hydrophobic CPC quencher; a static hydrophobic complex was formed.

The solution polymerization technique gave a pyrenesulfonamide-labeled copolymer, 2, with largely intramolecular associative behavior. Fluorescence measurements suggested this copolymer has a random microstructure, as would be expected to result from the copolymerization of two acrylamide monomers in a homogeneous medium. The random microstructure of this polymer appears to facilitate a compact conformation due to intramolecular hydrophobic interactions of the interspaced pyrenesulfonamide label. The Huggins profile of this polymer in aqueous solutions has zero slope, demonstrating a compact, noninteracting conformation. On a molecular level, I_E/I_M values are independent of polymer concentration,

paralleling the viscosity response of this system. Associations of the pyrene label are also static. Although the polymer conformation is compact, fluorescence quenching and lifetime measurements suggest the pyrenesulfonamide labels reside in a relatively aqueous microenvironment and are approached and encountered by small molecules at or near the diffusional rate. Quenching of this copolymer with the hydrophobic CPC confirmed the hydrophobic character of the pyrenesulfonamide label and its tendency to form static aggregates via hydrophobic associations in H_2O.

In summary, we have employed photophysical techniques to elucidate the associative behavior of pyrenesulfonamide-labeled polyacrylamides in aqueous media. Correlations between macroscopic (viscometric) and molecular (photophysical) characterization methods have allowed us to develop structure–property relationships for systems in which the pyrenesulfonamide moiety serves as the sole hydrophobe responsible for associative behavior.

Acknowledgment. Research support from DARPA, the Office of Naval Research, the Department of Energy, Unilever, and the National Science Foundation EPSCOR program is gratefully acknowledged.

References and Notes

(1) Herkstroeter, W. G.; Martic, P. A.; Hartman, S. E.; Williams, J. L. R.; Faird, S. *J. Polym. Sci., Polym. Chem. Ed.* **1983**, *21*, 2473.
(2) Chu, D. Y.; Thomas, J. K. *Macromolecules* **1984**, *17*, 2142.
(3) Turro, N. J.; Arora, K. S. *Polymer* **1986**, *27*, 783.
(4) Arora, K. S.; Turro, N. J. *J. Polym. Sci., Polym. Chem. Ed.* **1987**, *25*, 259.
(5) Stramel, T. D.; Nguyen, C.; Webber, S. E.; Rodgers, M. A. J. *J. Phys. Chem.* **1988**, *92*, 2934.
(6) Char, K.; Frank, C. W.; Gast, A. P.; Tang, W. T. *Macromolecules* **1987**, *20*, 1833.
(7) Winnik, F. M.; Winnik, M. A.; Tazuke, S.; Ober, C. K. *Macromolecules* **1987**, *20*, 38.
(8) Winnik, F. M. *Macromolecules* **1987**, *20*, 2745.
(9) Winnik, F. M. *Macromolecules* **1989**, *22*, 734.
(10) Winnik, F. M. *J. Phys. Chem.* **1989**, *93*, 7452.
(11) Winnik, F. M. *Langmuir* **1990**, *6*, 522.
(12) Winnik, F. M. *Macromolecules* **1990**, *23*, 233.
(13) Oyama, H. T.; Tang, W. T.; Frank, C. W. *Macromolecules* **1987**, *20*, 1839.
(14) Hemeker, D. J.; Garza, V.; Frank, C. W. *Macromolecules* **1990**, *23*, 4411.
(15) Oyama, H. T.; Hemeker, D. J.; Frank, C. W. *Macromolecules* **1989**, *22*, 1255.
(16) Nakaro, Y.; Komiyama, J.; Iijima, J. *Colloid Polym. Sci.* **1987**, *265*, 139.
(17) Horak, V.; Crist, D. R. *J. Chem. Ed.* **1975**, *52*, 665.
(18) Peer, W. J. In *Polymers in Aqueous Media*; Glass, J. E., Ed.; Advances in Chemistry Series 223; American Chemical Society: Washington, DC 1989; p 411.
(19) Dowling, K. C.; Thomas, J. K. *Macromolecules* **1990**, *23*, 1059.
(20) Israelachvili, J.; Pashley, R. *Nature* **1982**, *300*, 341.
(21) Israelachvili, J. *Acc. Chem. Res.* **1987**, *20*, 415.
(22) Char, K.; Frank, C. W.; Gast, A. P. *Macromolecules* **1989**, *22*, 3177.
(23) Avis, P.; Porter, G. *J. Chem. Soc., Faraday Trans. 2* **1974**, *70*, 1057.
(24) Birks, J. B. *Photophysics of Aromatic Molecules*; Wiley-Intersciences: New York, 1970; Chapter 7.
(25) Winnik, M. A.; Pekcan, O.; Egan, L. *Polymer* **1984**, *25*, 1767.
(26) Wang, F. W.; Lowry, R. E.; Cavanagh, R. R. *Polymer* **1985**, *26*, 1657.
(27) Char, K.; Gast, A. P.; Frank, C. W. *Langmuir* **1988**, *21*, 989.
(28) Kalyanasundaram, K. *Photochemistry in Microheterogeneous Systems*; Academic: Orlando, FL, 1987; p 126.
(29) Lakowicz, J. R. *Principles of Fluorescence Spectroscopy*; Plenum: New York, 1983; Chapter 9.
(30) Goddard, E. D. *Colloids Surf.* **1986**, *19*, 255.
(31) Breuer, M. M.; Robb, I. D. *Chem. Ind.* **1972**, 530.
(32) Chandar, P.; Somasundaran, P.; Turro, N. J. *Macromolecules* **1988**, *21*, 950.
(33) Winnik, F. M.; Ringsdorf, H.; Venzmer, J. *Langmuir* **1991**, *7*, 905.
(34) Winnik, F. M.; Ringsdorf, H.; Venzmer, J. *Langmuir* **1991**, *7*, 912.
(35) McCormick, C. L.; Ezzell, S. A. *Macromolecules*, previous paper in this issue.
(36) Chu, D.; Thomas, J. K. *J. Am. Chem. Soc.* **1986**, *108*, 6270.
(37) Ettink, M. R.; Ghiron, C. A. *J. Phys. Chem.* **1976**, *80*, 486.
(38) Ezzell, S. A. Ph.D. Dissertation, University of Southern Mississippi, Hattiesburg, MS, 1990.